SMiRT-12 / K. Kussmaul (Editor)

NON-LINEAR THERMAL AND STRUCTURAL ANALYSIS OF A TYPICAL SPENT FUEL SILO

L.M. Alvarez[1], G.R. Mancini[1], O.A.F. Spina[2], G. Sala[2] and F. Paglia[2]

[1]ENACE S.A., L.N. Alem 712, 1001 Buenos Aires, Argentina
[2]CNEA, Arribeños 3619, 1429 Buenos Aires, Argentina

ABSTRACT

A numerical method for the non-linear structural analysis of a typical reinforced concrete spent fuel silo under thermal loads is proposed.

The numerical time integration was performed by means of a time explicit axisymmetric finite-diference numerical operator. An analysis was made of influences by heat, visco-elasticity and cracking upon the concrete behaviour between concrete pouring stage and the first period of the silo's normal operation.

The following parameters were considered for the heat generation and transmission process:

* Heat generated during the concrete's hardening stage
* Solar radiation effects
* Natural convection
* Spent-fuel heat generation

For the modelling of the reinforced concrete behaviour, use was made of a simplified formulation of:

* Visco-elastic effects
* Thermal cracking
* Steel reinforcement

A comparison between some experimental temperature characteristic values obtained from the numerical integration process and empirical data obtained from a 1:1 scaled prototype was also carried out.

INTRODUCTION

Due to fundamental economical reasons, the Board of Directors of the Argentine National Atomic Energy Commission (CNEA) decided to encourage the development of a dry spent-fuel storage system to be used at the Embalse Nuclear Power (CNE), located in Río Tercero, Argentina. This NPP is a 648 MWe CANDU facility.

A conceptual basic design of the system was developed. This basic design was verified, under normal operating conditions, by testing a 1:1 scaled prototype silo placed next to the NPP site.

Simultaneously, a numerical method of analysis was developed. This model, adequately calibrated with test results, is being used to analyze abnormal operating conditions.

DESCRIPTION OF THE MATHEMATICAL MODEL

The following simplified mathematical notation is used:

$$\theta \quad \text{means} \quad \theta(R,\varphi,Z,t) \qquad [1]$$
$$\theta(\Delta R-\Delta t) \quad \text{means} \quad \theta(R+\Delta R,\varphi,Z,t-\Delta t)$$

The equation for heat transmission, referred to a system of cylindrical coordinates, is:

$$\frac{k}{c\rho}\cdot\left(\frac{\partial^2\theta}{\partial R^2}+\frac{1}{R}\frac{\partial\theta}{\partial R}+\frac{1}{R^2}\frac{\partial^2\theta}{\partial\varphi^2}+\frac{\partial^2\theta}{\partial z^2}\right)=\frac{\partial\theta}{\partial t} \qquad [2]$$

k : thermal conductivity coefficient
c : specific heat
ρ : mass density
θ : nodal temperature
R,φ,z : nodal cylindrical coordinates
t : time coordinate

An approximation to θ, by means of Taylor's expansion,

$$\theta(\Delta t)\approx\theta+\Delta t\cdot\frac{\partial\theta}{\partial t}+\frac{\Delta t^2}{2}\cdot\frac{\partial\left(\frac{\partial\theta}{\partial t}\right)}{\partial t} \qquad [3]$$

and the following related finite-difference operator were used for replacement:

$$\frac{\partial\left(\frac{\partial\theta}{\partial t}\right)}{\partial t}\approx\frac{\frac{\partial\theta}{\partial t}-\frac{\partial\theta(-\Delta t)}{\partial t}}{\Delta t} \qquad [4]$$

Then, the following equation is obtained by substituting eq. [4] into [3] and by further replacing $\partial\theta/\partial t$ by the first member in [2]:

$$\theta(\Delta t)=\theta+\frac{\Delta t\cdot k}{2c\rho}\cdot\left[3\cdot\left(\frac{\partial^2\theta}{\partial R^2}+\frac{1}{R}\cdot\frac{\partial\theta}{\partial R}+\frac{1}{R^2}\cdot\frac{\partial^2\theta}{\partial\varphi^2}+\frac{\partial^2\theta}{\partial z^2}\right)-\left(\frac{\partial^2\theta(-\Delta t)}{\partial R^2}-\frac{1}{R}\cdot\frac{\partial\theta(-\Delta t)}{\partial R}-\frac{1}{R^2}\cdot\frac{\partial^2\theta(-\Delta t)}{\partial\varphi^2}+\frac{\partial^2\theta(-\Delta t)}{\partial z^2}\right)\right] \qquad [5]$$

This equation makes it possible to extrapolate the temperatures corresponding to an instant t + Δt. Their time integration was carried out by using the well-known central finite-diference operators[1]:

$$\frac{\partial\theta}{\partial R}\approx\frac{\theta(+\Delta R)-\theta(-\Delta R)}{2\Delta R} \qquad [6]$$

$$\frac{\partial^2\theta}{\partial R^2}\approx\frac{\theta(-\Delta R)-2\theta+\theta(\Delta R)}{\Delta R^2}$$

$$\frac{\partial^2\theta}{\partial\varphi^2}\approx\frac{-\theta(-2\Delta\varphi)+16\theta(-\Delta\varphi)-30\theta+16\theta(\Delta\varphi)-\theta(2\Delta\varphi)}{12\Delta\varphi^2}$$

$$\frac{\partial^2\theta}{\partial z^2}\approx\frac{-\theta(-2\Delta z)+16\theta(-\Delta z)-30\theta+16\theta(\Delta z)-\theta(2\Delta z)}{12\Delta z^2}$$

Similar mathematical expressions were used for expanding (-Δt).
The inner cylinder boundary condition is:

$$Q_i+k\cdot\left(\frac{\partial\theta}{\partial R}\right)_{R=R\,int}=0$$

Q_i : Heat generated by the fuel-spent elements [7]

R_{int} : inner cylinder radius

The outer cylinder boundary condition is:

$$h(\theta_a - \theta) - \mathcal{J}\sigma(\theta + 273)^4 + Qs - k\left(\frac{\partial\theta}{\partial R}\right)_{(R=R_{ext})} \qquad [8]$$

h : thermal convection coefficient
θ_a : external air temperature
$\mathcal{J}$: radiation factor
σ : Stefan Bolzmann constant
Q_S : solar radiation
R_{ext} : outer cylinder radius

The surrounding air temperature can be assumed by means of an approximate law like:

$$\theta_a(t) = \frac{1}{2}\left\{\theta_{min} + \theta_{max} + (\theta_{min} - \theta_{max})\cos\left[\frac{\pi}{12}(t - t_{cal})\right]\right\} \qquad [9]$$

θ_{min} : minimum daily air temperature
θ_{max} : maximum daily air temperature
t_{cal} : site specific calibration angle

Several other site-specific functions of the daily temperature variation can be equally defined.

The theoretical solar radiation, Q_s, was defined as:

$$Q_s(t) = Q_{sn} \cdot \cos(\gamma_{h(t)} - \varphi_p) \cdot \cos[\gamma_{v(t)}] \qquad [10]$$

Q_{sn} : normal solar radiation per unit of time
$\gamma_{h(t)}$: horizontal angle defining the apparent movement of the sun
φ_p : horizontal angle defining a specific external boundary point (the same angle reference used for $\gamma_{h(t)}$ must be applied)
$\gamma_{v(t)}$: sets the specific sun elevation angle

The Q_{sn} functions used in the above equation are:

$$Q_{sn}\left[\frac{Kcal}{m^2 hour}\right] = 31.139 \cdot \gamma_v - 0.41722 \cdot \gamma^2{}_v + 0.0018889 \cdot \gamma^3{}_v \qquad [11]$$

for $\gamma_v \leq 50$ degrees

$$Q_{sn}\left[\frac{Kcal}{m^2 hour}\right] = 39.286 \cdot \gamma_v - 0.67619 \cdot \gamma^2{}_v + 0.0038095 \cdot \gamma^3{}_v$$

for $\gamma_v > 50$ degrees

The approximate formulas of the time variation of horizontal and vertical angles, used to refer the apparent movement of the sun, are described below. They were referred to an orthogonal set of coordinates with +x axis oriented as the geographic north and +z axis normal to the site's horizontal plane.

$$\alpha = 0.4092797 \cdot \sin[0.017214 \cdot (N_d - 80)] \qquad [12]$$

$$\beta = 0.261799 \cdot (\text{hour} - 12)$$
$$(0 \leq \text{hour} \leq 24)$$

$$x = \cos(\alpha) \cdot \cos(\beta) \cdot \sin(\alpha_{lat}) - \sin(\alpha) \cdot \cos(\alpha_{lat})$$
$$y = \cos(\alpha) \cdot \sin(\beta)$$
$$z = \cos(\alpha) \cdot \cos(\beta) \cdot \cos(\alpha_{lat}) + \sin(\alpha) \cdot \sin(\alpha_{lat})$$

α,β : reference angles
Nd : number of days sence January 1st
hour : hour of the day (0 to 24 should be used)
αlast : site latitude
x,y,z : reference coordinates for apparent sun position

$$\gamma_h(t) = tg^{-1}\left(\frac{x}{y}\right)$$

$$\gamma_v(t) = \sin^{-1}\left[\frac{z}{\left(x^2 + y^2 + z^2\right)^{1/2}}\right]$$

The outer boundary condition was solved by the iterative Newton-Raphson method.
The thermal convection coefficient was obtained from the following empirical formula:

$$h = c_1 + c_2\sqrt{v_w} \qquad [13]$$

c_1, c_2: calibration coefficients
v_w : wind speed

where c_1 and c_2 must be adequately calibrated for each specific site, although other formulas may also be successfully employed.

The concrete hardening stage was analyzed on the basis of concrete properties obtained from local materials.(2) The heat generated by chemical reactions between the water and the components of concrete was obtained from experimental values of local materials (see Fig. 1) and used in the thermal equilibrium equation as an additional term:

$$\theta_c = \theta + Q_{ch} \cdot (t - t_p) \cdot M_c \cdot \Delta t \qquad [14]$$

θ_c : corrected nodal temperature
$Q_{ch} \cdot (t - t_p)$: instant heat generated by chemical reactions
t_p : reference time of concrete pouring stage
Δt : numerical integration time step

The assessment of thermal stress and strain generated in the cylinder structure was carried out by means of a standard non-linear finite-element method. The elasticity modulus of the compressed concrete was reduced by a coefficient in accordance with that proposed by the CEB.(3)

The appearance of structural cracking was controlled by comparing the principal tensile stresses vs concrete maximum tensile capacity. Wherever cracking state was detected, the concrete elasticity modulus was reduced by a normative factor that is calibrated by the amount of reinforcement, the distance between cracks and the maximum steel reinforcement

bond stresses.(4)(5)

The results from the application of the proposed mathematical methodology were compared with the data obtained from the prototype described below and adjusted accordingly. The time evolution of the mean temperature of the reinforced concrete was registered as from pouring time. Then, comparisons were made for two specific spots (t1 and t2), 40 hours apart, since it was in that period that the first cracking appeared.

DESCRIPTION OF THE PROTOTYPE SILO

Geometrical and mechanical properties

The geometrical characteristics and the mechanical and physical properties of the prototype were adopted principally to obtain a good radiation protection shielding and thermal dissipation. The most relevant structure dimensions and material properties are described in Fig. 2 and in Tables 1 and 2.

Instrumentation

Two types of fundamental magnitudes (temperature and strain) were measured by using three different types of instruments:

* K-Type thermocouples
* Strain gauges (five 10-unit sets)
* SC-2 vibrating wire strain gauges

Over 150 different measuring instruments were installed.

The thermal loads were produced by three heaters with a maximum total power capacity of 8 KWh. The distribution of heaters conditioned the relative position of the measuring instruments. A maximum area of coverage was procured.

DESCRIPTION OF THE TEST

Sequence of thermal loads

The original test was programmed as a sequence of alternative stages of stationary power supply, followed or preceded by non-stationary peaks. Part of the most significant measured values during the test are shown in Fig. 3. The first cracking was detected at mid height of the external face, during the second non-stationary thermal period.

Measured values

The significant values described in Figs. 4 and 5 correspond with actual registered temperatures in different positions of the above referenced middle plane. These values are compared in the same figures with the theoretical results obtained through the proposed numerical method.

FINAL REMARKS

A numerical method for analyzing heat evolution in time of a spent fuel silo was developed and good agreement with experimental results was obtained.

Some small differences between readings and the calculated values can be partially explained by possible accidental movements of the measuring instruments (by human error or during the pouring of concrete).

The influence of cracking upon the reduction of thermal stress was significant, while visco-elastic effects were less relevant.

The numerical processing of the developed explicit finite-difference method is very fast. A computer code was developed for running in a 25 Mhz 486 PC and it was found that only 3 seconds were needed for each step of nodal temperature extrapolation (in a reference system of 1200 nodes).

ACKNOWLEDGMENTS

The authors are specially thankful to the members of CNEA's EECE and Thermohydraulics teams for their cooperation in several tasks related to the contents of this paper.

REFERENCES

1. Brush, D.O. and Almroth, B.O., 1975. *"Buckling of bars, plates and shells"*, Mc

Graw Hill, p. 278.
2. Balado, J.F.G., *"Método para la dosificación de hormigones"*, Instituto Argentino de Cemento Portland, Boletín N° 42 Serie E4, Buenos Aires.
3. Chiorino, M.A., 1972. *"Effets structuraux des deformations différées du beton"*, CEB, Bulletin N° 80.
4. Montoya, P.J.; Meseguer, A.G. and Cabre, F.M., *"El hormigón armado"*, Ed. G. Gili, Tomo I, p. 437-442.
5. Comité Euro-International du Beton, 1977. *"Systéme International de Reglementation Technique Unifiée des Structures - Volume II - Code Modele CEB-FIP pour les structures en beton"*, Bulletin D'Information N° 125.
6. Instituto Argentino de Racionalización de Materiales, 1974. *"Norma IRAM 11601"*.
7. Bonzel, J. *"Beton Kalender"*, Ed. Verlag von Wilheim Ernst & Sohn, Berlin-Munich.
8. Instituto Nacional de Prevención Sísmica, 1983. *"Proyecto, cálculo y ejecución de estructuras de hormigón armado y pretensado"*, INPRES-CIRSOC 201.

Table 1. Concrete Properties [6][7][8]

Weight density	2.3 Kg/dm^3
Water/Cement ratio	0.53
Coefficient of thermal conduct	1.75 Kcal/m.°C.h
Reinforcement/Concrete ratio	250 Kg/m^3

Table 2. Reinforcement Properties [7][8]

Weight density	7800 Kg/dm^3
Modulus of Elasticity	2100000 Kg/cm^2
Coefficient of thermal conduct	1.75 Kcal/m.°C.h
Yield Strength	4200 Kg/cm^2
Modulus of Poisson	0.3

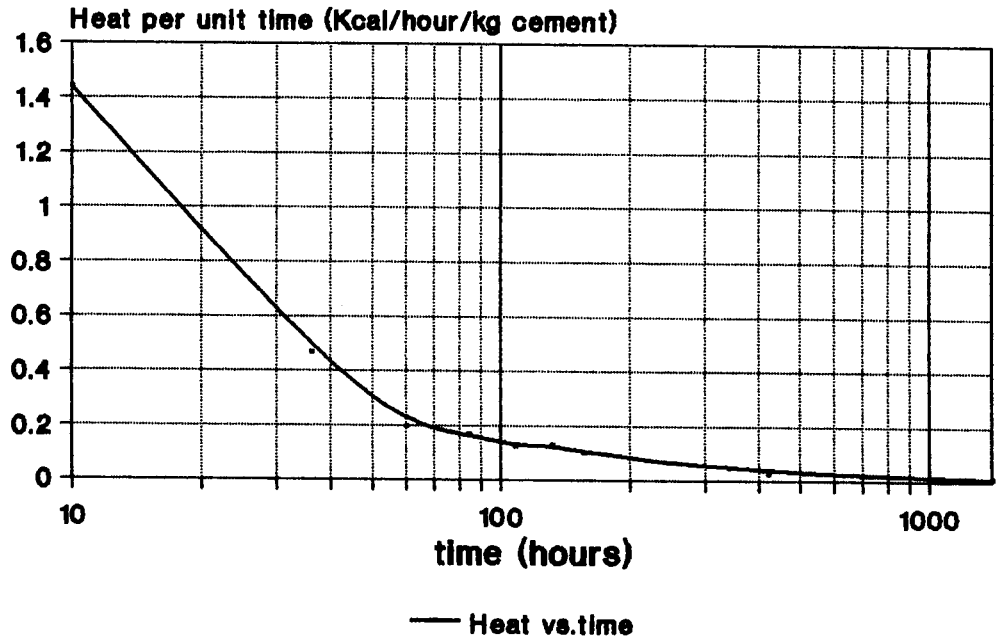

Fig. 1 - Heat generated by water-cement chemical reactions per unit of time

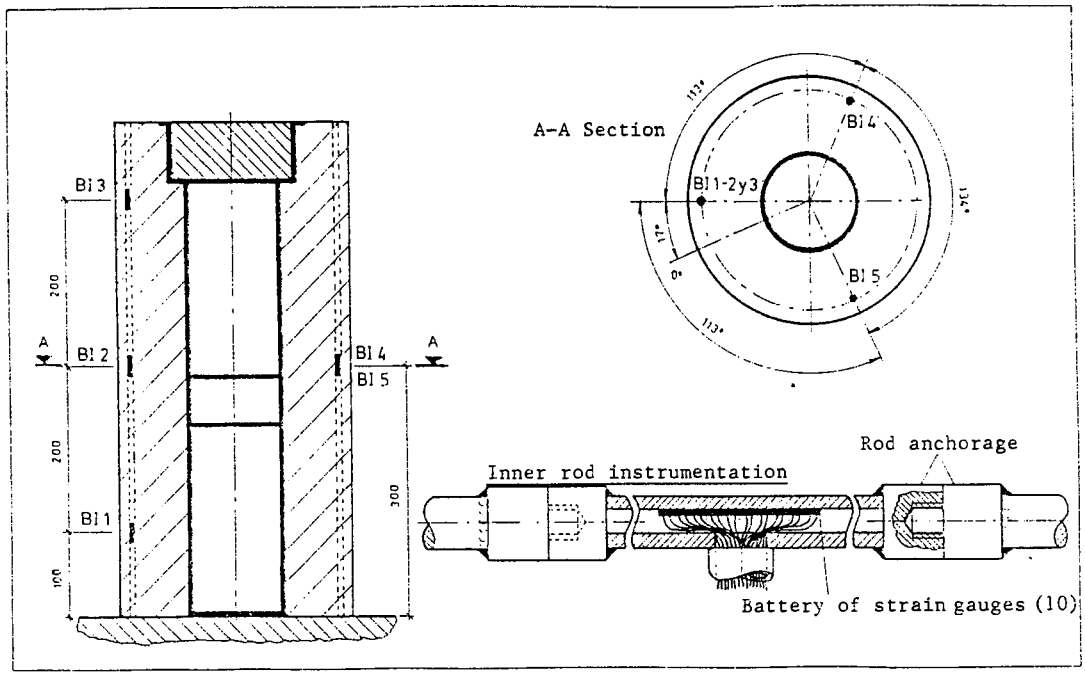

Fig. 2 (a) Positioning of strain gauges

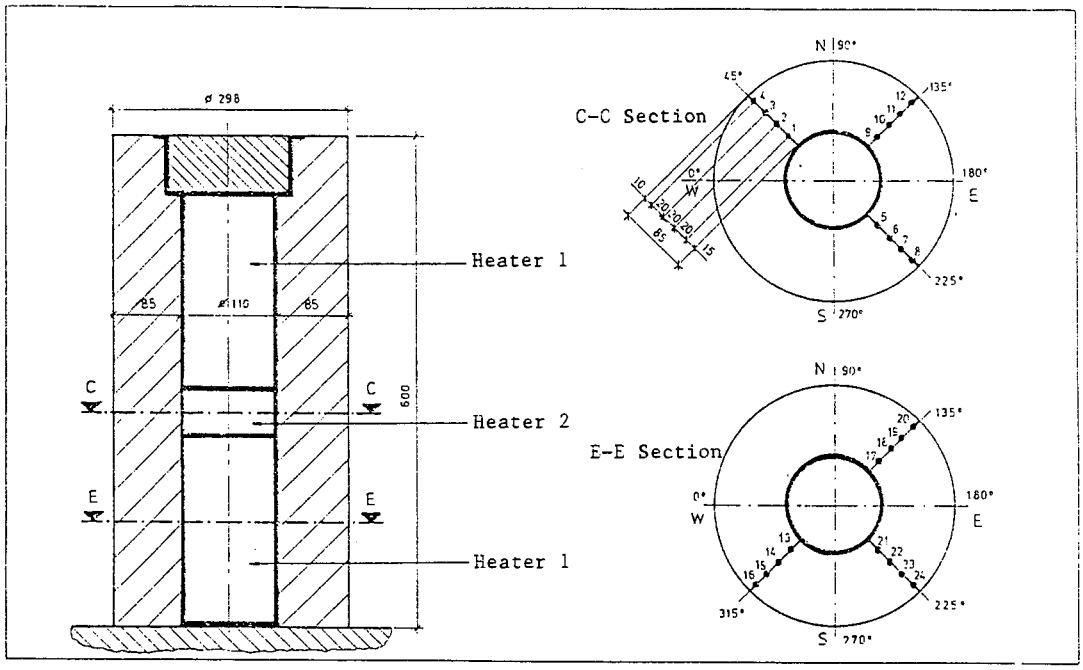

Fig. 2 (b) Positioning of thermocouples and heaters

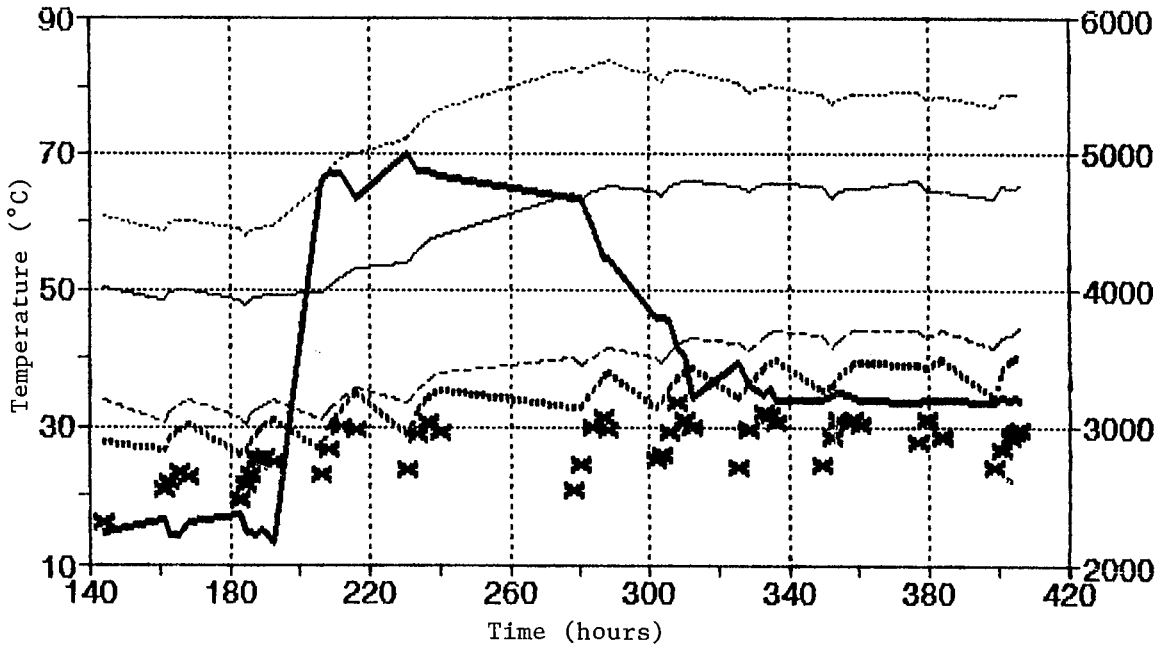

Fig. 3 - Temperature evolution in the mid plane

15 cm
35 cm
55 cm
75 cm
Room temperature
Power

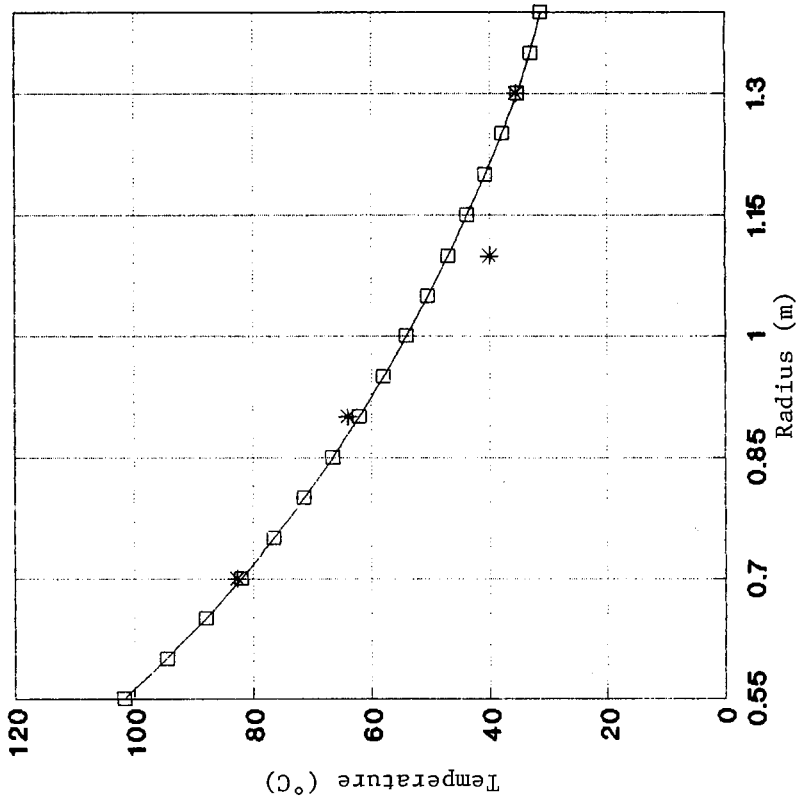

Fig. 5 - Comparison of mid-plane average temperatures. (time: 280 hours)

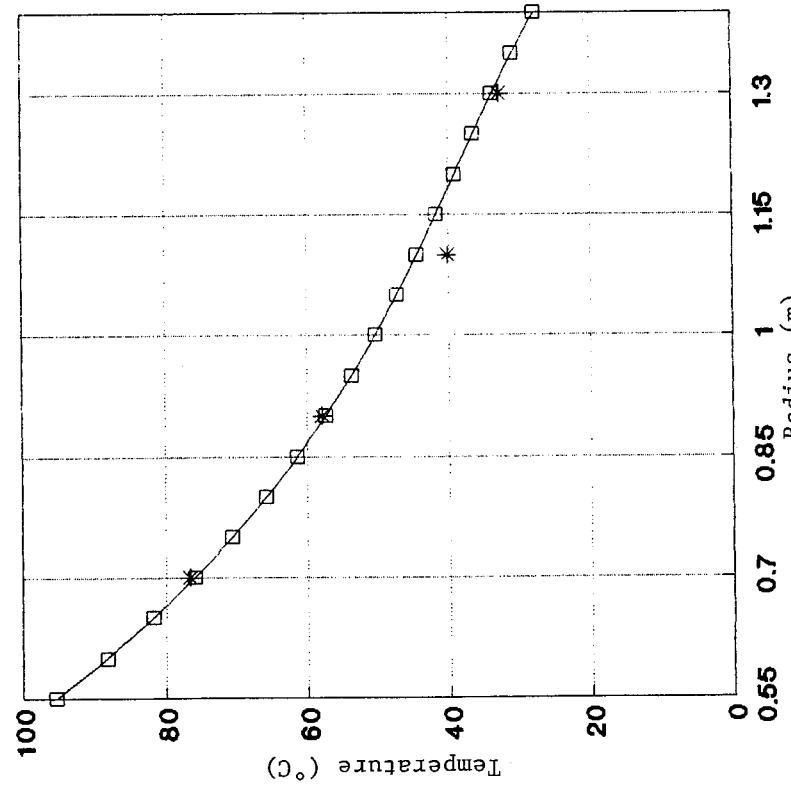

Fig. 4 - Comparison of mid plane average temperatures. (time: 240 hours)